

## AMP-activated protein kinase controls metabolism and heat production during embryonic development in birds

Isabel Walter<sup>1</sup>, Bronwyn Hegarty<sup>2</sup> and Frank Seebacher<sup>1,\*</sup>

<sup>1</sup>School of Biological Sciences A08, Integrative Physiology, University of Sydney, Sydney, NSW 2006, Australia and <sup>2</sup>Garvan Institute of Medical Research, Sydney, NSW 2010, Australia

\*Author for correspondence (frank.seebacher@sydney.edu.au)

Accepted 16 June 2010

### SUMMARY

**During embryonic and early juvenile development, endotherms must balance energy allocation between growth and heat production. Failure to either match the ATP demand of growing tissue or produce heat at the correct developmental stage will lead to damage of the organism. We tested the hypothesis that AMP-activated protein kinase (AMPK) is involved in the regulation of energy metabolism and heat production during development in the chicken (*Gallus gallus*). We show that mRNA concentrations of regulatory and catalytic AMPK subunits, AMPK total protein, and AMPK phosphorylation increase during development [3 days (–3 days) and one day (–1 day) before hatching, and +1 day and +8 days after hatching] in liver, and to a lesser extent in skeletal muscle. Chronic stimulation with 5-aminoimidazole-4-carboxamide-1-β-D-ribofuranoside (AICAR) significantly increases AMPK phosphorylation in skeletal muscle and in liver. This increase was paralleled by significant increases in heat production, glucose utilization, and liver and skeletal muscle mitochondrial capacity (citrate synthase activity). The effects of AMPK are likely to be mediated by inhibition of acetyl CoA carboxylase (ACC) after hatching, when ACC protein concentration increases significantly, and by a significant AMPK-induced increase in PGC-1α mRNA concentration (at +1 day), but not in NRF-1 mRNA concentration. AMPK phosphorylation is under the control of thyroid hormone, and AMPK phosphorylation decreases significantly following the induction of hypothyroidism. We propose AMPK as a principal regulatory mechanism during the transition from ectothermy to endothermy in birds, and show that AMPK function in birds is similar to that observed in mammals.**

Key words: thermoregulation, mitochondria, PGC-1α, thyroid hormone, ACC, endothermy.

### INTRODUCTION

The transition from ectothermy to endothermy during ontogenetic development in endotherms is facilitated by an increase in mitochondrial density and enzyme activities in oxidative pathways, which leads to an increase in oxidative metabolic capacity (Seebacher et al., 2006; Walter and Seebacher, 2007). Increased mitochondrial metabolic flux is at least partly driven by increasing cellular ATP demands caused by elevated Na<sup>+</sup>/K<sup>+</sup>-ATPase activity (Walter and Seebacher, 2009; Wu et al., 2004). At the same time mitochondria become more uncoupled (Walter and Seebacher, 2009). Together, these processes can increase metabolic heat production but reduce the efficiency of ATP synthesis (Brand et al., 1991; Else and Hulbert, 1987; Hulbert and Else, 1990). Therefore, the development of endothermy exposes the growing organism to an energy allocation challenge, between growth and heat production, which requires a regulatory mechanism to match ATP production with ATP usage. Understanding these as yet unknown regulatory mechanisms will significantly advance understanding of energetic allocation during endothermic development by providing the biological mechanisms underlying theoretical models of ontogenetic energy budgets (Hou et al., 2008; Kooijman et al., 2008). We propose that metabolic co-ordination during development is achieved by AMP-activated protein kinase (AMPK).

AMPK is one of the major cellular energy sensors (Carling et al., 2008) and an intracellular low-energy warning system (Hardie and Carling, 1997; Hegarty et al., 2009). AMPK is a serine/threonine kinase with heteromeric structure, composed of a catalytic alpha and regulatory beta and gamma subunits (Hardie and Carling, 1997).

In situations of high ATP use, AMP levels increase and activate AMPK (Kahn et al., 2005) by promoting net phosphorylation of the Thr172 residue on the α subunit, and also by allosteric activation of phosphorylated AMPK (Sanders et al., 2007; Winder and Thomson, 2007). Additionally, AMPK phosphorylation might be regulated by hormones (for example, by thyroid hormones) to control metabolic pathways and mitochondrial biogenesis (Irrcher et al., 2003). Once activated, pAMPK can phosphorylate a variety of downstream targets, which can lead to an increase in the rate of fatty acid oxidation and ATP generation, and to decreased rates of energy utilization (Hardie and Carling, 1997).

As an immediate action to restore cellular energy charge, AMPK enhances the availability of carbohydrates and fats as fuels for mitochondrial oxidation to produce ATP. As one of its main targets, pAMPK phosphorylates acetyl CoA carboxylase (ACC), thereby blocking fat storage and promoting fatty acid oxidation in mitochondria (Winder and Thomson, 2007). In addition to this acute (1–2 h) regulation, AMPK is involved in long-term (over several days) regulation of ATP production. Thus, AMPK controls mitochondrial biogenesis by increasing the abundance of the transcriptional co-activator PGC-1α (Irrcher et al., 2003; Reznick and Shulman, 2006), and by activating nuclear respiratory factor-1 (NRF-1) (Bergeron et al., 2001; Zong et al., 2002). PGC-1α is a prominent metabolic regulator in mammals (Finck and Kelly, 2006; Puigserver and Spiegelman, 2003), and it has recently been shown to play a role in the metabolic regulation of birds (Walter and Seebacher, 2007). Hence, because of its potential to modulate mitochondrial capacity and thereby heat production and ATP

availability, AMPK possesses the right characteristics to act as a metabolic regulator during the embryonic development of endothermy.

The aim of this study was to determine whether AMPK controls metabolic capacity and heat production during ontogenetic development of birds. We tested the hypotheses that chronic AMPK activation boosts endothermic heat production and increases the oxidative capacity of mitochondria, and that thyroid hormones coordinate these events *via* their regulatory effect on AMPK activation.

## MATERIALS AND METHODS

### Animals

All procedures were approved by the University of Sydney Animal Ethics Committee (Approval Number: L04/11-2008/1/4922). We used chicken embryos as model system because of the well established transition from ectothermy to endothermy; during development embryos are ectothermic and cannot regulate their body temperature metabolically, but chicks become endothermic by eight days after hatching (Decuypere, 1984; Tzschentke and Nichelmann, 1999). Fertilized chicken eggs (*Gallus gallus*) were obtained from a local supplier (Cordina Chicken Farms, Sydney, Australia). Eggs were incubated at a constant temperature (38°C) and relative humidity (60–67%; Octagon 40 Incubator, Brinsea Products, Sandford, North Somerset, UK). Internal pipping occurred on day 19/20 and hatching on day 20/21 of incubation. After hatching the hatchlings were transferred to an enclosure in a temperature-controlled room (23.0±2.0°C), and were provided with heating lamps, and with water and commercial chicken starter feed *ad libitum*. In all experiments, embryos were staged using the Hamburger and Hamilton (HH) system (Hamburger and Hamilton, 1951) and were weighed to confirm that treatment groups were equal in development (Walter and Seebacher, 2009).

Tissue samples (from  $N=6-8$  birds per time point) were collected three days before hatching (referred to as -3), one day before hatching (-1), one day after hatching (+1) and eight days after hatching (+8). Animals were euthanized by cervical dislocation. Breast muscle (*musculus pectoralis*) and liver were collected, frozen in liquid nitrogen for enzyme and western blot analyses, or harvested in RNAlater (Ambion, Austin, TX, USA) for mRNA analyses.

### Acute AMPK activation

AMPK phosphorylation has previously been pharmacologically induced *via* AICAR administration in mammals (5-aminoimidazole-4-carboxamide-1- $\beta$ -D-ribofuranoside; Toronto Research Chemicals, Toronto, ON, Canada). However, to the best of our knowledge AICAR has not been tested in birds before. Therefore, we tested two AICAR concentrations, which are commonly used in rodent models (Halseth et al., 2002; Winder et al., 2000), to determine whether we could activate AMPK in birds during development. On day 17 of incubation, we injected embryos with 0.5 mg g<sup>-1</sup> bodyweight AICAR (0.5 mg AICAR group;  $N=8$ ), 1 mg g<sup>-1</sup> bodyweight AICAR (1 mg AICAR group;  $N=8$ ) or a physiological saline solution (control group;  $N=8$ ). A hole was made in the eggshell with a needle and all injections were given in the yolk. After the procedure the eggshell was sealed with Parafilm (Parafilm M, Livingston, Rosebery, Australia). Tissue samples were collected one hour after treatment.

### Chronic AMPK activation

For chronic AMPK activation, starting on day 16 of incubation, chicken embryos were injected in the yolk daily [three injections]

with 1 mg g<sup>-1</sup> bodyweight of AICAR dissolved in physiological saline (AICAR group;  $N=16$ ) or with a physiological saline solution (control group;  $N=16$ ). To avoid an acute effect of AICAR, animals were not injected with AICAR or with the control solution on the day of sample collection. Tissue samples were collected one day before hatching (-1; control group,  $N=8$ ; AICAR group,  $N=16$ ) and one day after hatching (+1; control group,  $N=8$ ; AICAR group,  $N=16$ ). Oxygen consumption (please see below) of all animals was measured immediately before samples were collected on days -1 and +1. Plasma glucose levels were determined using a glucose analyser (TrueTrack, DiaCare, Diabetes Association of Australia, Willoughby, NSW, Australia) at the time of sample collection.

### Alteration of thyroid hormone levels

To induce hypothyroidism, embryos were injected on day 14 of incubation with 1.5 mg methimazole (Walter and Seebacher, 2009) dissolved in physiological saline (hypothyroid group;  $N=12$ ) or with a physiological saline solution alone (control group;  $N=12$ ). We established previously that this methimazole treatment significantly reduced thyroid hormone concentrations (Walter and Seebacher, 2009). Tissue samples were collected one day before hatching (-1).

### Closed system respirometry

The rate of oxygen consumption ( $\dot{V}_{O_2}$ ) of embryos one day before hatching was measured using standard closed system respirometry at a test temperature of 38°C. Individual eggs were placed in a 250 ml gas-tight plastic container in a temperature-controlled room. Initial (before sealing the chamber) and final (after 30 min) air samples (60 ml) were collected and their oxygen concentration measured with an oxygen electrode (Clark type, Rank Brothers, Cambridge, UK) connected to a computerized recording system (Powerlab 4S; AD Instruments, Bella Vista, Australia). After testing, eggs were weighed and their volume was measured *via* water displacement to subtract the egg volume from the container volume.  $\dot{V}_{O_2}$  (ml h<sup>-1</sup>) was calculated as (Hoyt et al., 1978):

$$\dot{V}_{O_2} = [\text{STPD} \times V \times (\Delta P_{O_2} / 100)] / [(1 - \text{FeO}_2) \times t], \quad (1)$$

where STPD is standard temperature and pressure, dry (denoting a volume of dry gas at 0°C and a pressure of 760 mmHg);  $V$  is the volume (250 ml) of the plastic container minus the displacement of the egg (ml);  $\Delta P_{O_2}$  is the initial oxygen concentration minus the final oxygen concentration (%);  $\text{FeO}_2$  is the fractional oxygen concentration in air (unitless);  $t$  is time (h).

### Open flow respirometry

Oxygen consumption of individual hatchlings was measured in an open respirometry system located in a temperature-controlled room. Birds were placed in a gas-tight plastic container (800 ml) fitted with an inlet and outlet for air. Incoming airflow was supplied by a pump (Applied Electrochemistry, Pittsburgh, PE, USA) with a constant flow of 210 ml min<sup>-1</sup> and passed through a spirometer (MK2; AD Instruments, Bella Vista, Australia). The outflowing gases passed through a drying column (MLA0343; AD Instruments, Bella Vista, Australia), and were monitored by a calibrated O<sub>2</sub> gas analyzer (ML205 Gas Analyser; AD Instruments). Data were collected with a computerized recording system (Powerlab 4S, AD Instruments).

Resting oxygen consumption was recorded continuously for 1.5–2 h at thermoneutral ambient temperature (35°C) (Bech et al., 1984; Klaassen et al., 1987). Resting oxygen consumption (RMR; ml h<sup>-1</sup>) was defined as the lowest rate of oxygen consumption maintained over 5 min and calculated as the mean of all data points collected over that period.

Heat production (HP;  $\text{mWembryo}^{-1}$ ) was calculated for both closed and open respirometry according to Heldmaier (Heldmaier, 1975):

$$\text{HP} = (4.44 + 1.43 \times \text{RQ}) \times M, \quad (2)$$

where RQ is the respiratory quotient ( $\text{CO}_2/\text{O}_2$ ), which we assumed to be 0.72 (Decuyper, 1984; Decuyper et al., 1979), and  $M$  is the  $\text{O}_2$  consumption ( $\text{ml h}^{-1}$ ).

#### mRNA concentrations

RNA was extracted from 40–100 mg of liver and muscle samples using TRIreagent (Molecular Research Centre, Cincinnati, OH, USA), following the manufacturer's instructions. RNA quality and concentration were verified using a Bioanalyzer (Agilent Biotechnologies, Palo Alto, CA, USA). One microgram of total RNA was treated with DNase I (Sigma, Castle Hill, NSW, Australia) and reverse-transcribed using RNase H-MMLV reverse transcriptase (Bioscript, Boline, London, UK) and random hexamer primers (Boline, London, UK).

Quantitative RT-PCR was performed on an Applied Biosystems 7500 qRT-PCR machine (Applied Biosystems, Scoresby, VIC, Australia) according to published protocols (Seebacher et al., 2006). Primer and dual label probes were designed from sequences obtained from GenBank for AMPK subunits  $\alpha 1$ ,  $\alpha 2$ ,  $\beta 2$ ,  $\gamma 1$  and  $\gamma 3$ , nuclear respiratory factor-1 (NRF1) and peroxisome proliferator activated receptor  $\gamma$  coactivator-1 alpha (PGC-1 $\alpha$ ). RNA polymerase II polypeptide E (POLR2E) was used as a housekeeping gene (Table 1). We measured the mRNA levels of AMPK subunits  $\alpha 1$ ,  $\beta 2$  and  $\gamma 1$  in liver and of AMPK subunits  $\alpha 2$ ,  $\beta 2$  and  $\gamma 3$  in skeletal muscle, because these genes are expressed predominantly in those tissues, respectively (Proszkowiec-Weglarz and Richards, 2007; Proszkowiec-Weglarz and Richards, 2009). Real-time PCR reactions with dual-labelled probes contained  $1 \times$  Immomix (Boline, London, UK),  $4.5 \text{ mmol l}^{-1}$   $\text{MgCl}_2$ ,  $50\text{--}900 \text{ nmol l}^{-1}$  primer and probe,  $1 \times$  ROX reference dye (Invitrogen, USA), and  $\sim 50 \text{ ng}$  cDNA. The cycle consisted of  $95^\circ\text{C}$  for 7 min, 40 cycles of  $95^\circ\text{C}$  for 20 s,  $60^\circ\text{C}$  for 1 min. Real-time PCR reactions with Sybr green contained  $1 \times$  SensiMixPlus SYBR (Quantace, London, UK),  $4.5 \text{ mmol l}^{-1}$   $\text{MgCl}_2$ ,  $50\text{--}900 \text{ nmol l}^{-1}$  primer and  $\sim 50 \text{ ng}$  cDNA. The cycle

consisted of  $95^\circ\text{C}$  for 7 min, 40 cycles of  $95^\circ\text{C}$  for 20 s,  $60^\circ\text{C}$  for 1 min. Dissociation curve analysis was performed after the amplification step to verify the presence of only a single PCR product. Relative mRNA concentration of the eight target genes at each stage of development and of AICAR treatments was calculated according to Pfaffl (Pfaffl, 2001), and normalized with POLR2E. As controls, we used adult chicken samples ( $N=6$ ) to assess changes in mRNA concentration during development, and the grand mean of all samples for each tissue for acute and chronic AMPK activation.

#### Western blot analyses

Samples of liver and muscle were homogenized in ice-cold lysis buffer containing  $50 \text{ mmol l}^{-1}$  HEPES, 10% v/v glycerol,  $1 \text{ mmol l}^{-1}$  EDTA,  $50 \text{ mmol l}^{-1}$  sodium fluoride,  $5 \text{ mmol l}^{-1}$  sodium pyrophosphate,  $1 \text{ mmol l}^{-1}$  dithiothreitol,  $100 \mu\text{M}$  PMSF and  $1 \times$  complete protease inhibitors (Roche, Castle Hill, Australia) and were left for 1 h at  $4^\circ\text{C}$  with gentle mixing. Lysates were cleared by centrifugation ( $13,000 \text{ g}$ , 10 min) and protein content determined with a Bradford assay (BioRad, Hercules, CA, USA). Lysates were mixed with loading buffer containing a final concentration of  $20 \text{ mmol l}^{-1}$  DTT and 2% (w/v) SDS and left to denature at room temperature for 1 h. Aliquots containing  $20\text{--}40 \mu\text{g}$  of protein were separated by SDS-PAGE using 10% acrylamide gels and then transferred to PVDF membranes. After blocking (5% skim milk in TBS-0.05% Tween, 60 min at room temperature), membranes were incubated overnight at  $4^\circ\text{C}$  with primary antibodies (1:1000 dilution) raised against total or phosphorylated (Thr 172) AMPK  $\alpha$  subunit, total or phosphorylated (Ser 79) ACC (all from Cell Signalling Technology, Beverly, MA, USA) or pan-14-3-3 (Santa Cruz Biotechnology, Santa Cruz, CA, USA). Following incubation with the appropriate HRP-conjugated secondary antibodies (1:10,000 dilution), protein bands were visualized using either Western Lightning (Perkin Elmer, Glen Waverley, VIC, Australia) or SuperSignal West Dura (Pierce, Rockford, IL, USA) enhanced chemiluminescent substrates and exposed to film (FujiFilm, Super RX). Signal intensities were determined by densitometric analysis using Odyssey IR imaging system software (LI-COR Biosciences, Lincoln, NE, USA) and normalized for 14-3-3. ACC and pACC

Table 1. Primer and dual-label probes designed from sequences obtained from GenBank

Accession No.	Primer and probe	Sequences
NM_001039603	AMPK subunit $\alpha 1$ -F	5'-ACGTCTGTCCAGCAAATCC-3'
NM_001039605	AMPK subunit $\alpha 1$ -R	5'-TTCTGGGCCTGCATATAACC-3'
	AMPK subunit $\alpha 2$ -F	5'-AGCACGCCAACAGACTTCTT-3'
	AMPK subunit $\alpha 2$ -R	5'-CAGCACGTTCTCTGGTTTCA-3'
NM_001044662	AMPK subunit $\beta 2$ -F	5'-CCTGGAGGAGTCTGTGAAGC-3'
	AMPK subunit $\beta 2$ -R	5'-GGTCCAGGATAGCGACAAAG-3'
XM_001236051	AMPK subunit $\gamma 1$ -F	5'-AGCTGCAGATCGGTACCTACA-3'
NM_001031258	AMPK subunit $\gamma 1$ -R	5'-GGTCTTCTCAGCTGCCAAAT-3'
	AMPK subunit $\gamma 3$ -F	5'-GCCTGTCTATTGAACCCATCT-3'
	AMPK subunit $\gamma 3$ -R	5'-CCAGAGCAGCATACACAGGA-3'
NM_001030646	NRF1-F	5'-CTGTGTCCCTCATCCAGGTT-3'
	NRF1-R	5'-AGTTCTGCTCCACCTCTCCA-3'
NM_001006457	PGC-1 $\alpha$ -F	5'-GACGTATCGCCTTCTTGCTC-3'
	PGC-1 $\alpha$ -R	5'-CTCGATCGGGAATATGGAGA-3'
	PGC-1 $\alpha$ probe	5'-(FAM)CCTCAACGCAGGCTTTGTTCCCG(BHQ1)-3'
XM_418224	POLR2E-F	5'-CATGCAGGAGGAGAACATCA-3'
	POLR2E-R	5'-TGCAGAACTGCTCCAGGAT-3'
	POLR2E probe	5'-(cy5)TGCTGCACCACAATCAGCGCACG(BHQ1)-3'

AMPK, AMP-activated protein kinase; F, forward; R, reverse.

were measured as one of the principal targets of AMPK in liver only. Due to antibody limitation, we could not detect total AMPK protein at -3 d in liver. pAMPK protein concentration was measured as a proxy for AMPK activity (Sanders et al., 2007).

### Enzyme assays

We assayed activities of cytochrome *c* oxidase (COX) and citrate synthase (CS) as indicators of mitochondrial oxidative capacity and abundance, respectively (Hoppeler, 1986). Liver and muscle tissue samples (approximately 50 mg) were homogenized in nine volumes of 50 mmol<sup>-1</sup> imidazole/HCl, 2 mmol<sup>-1</sup> MgCl<sub>2</sub>, 5 mmol<sup>-1</sup> EDTA, 1 mmol<sup>-1</sup> reduced glutathione and 0.1% Triton X-100. All assays were conducted at 38°C, according to published protocols (Seebacher et al., 2003).

### Statistical analysis

Data are presented as means ± s.e.m. mRNA and protein concentration data for different stages of development were analyzed by one-way ANOVA followed by LSD pairwise comparison. We compared acute AICAR, chronic AICAR, and hypothyroid treatments with their respective control treatments by two-tailed *t*-tests for independent samples, except that we used a one-tailed *t*-test when we explicitly tested for an increase in PGC-1 $\alpha$  mRNA concentration and in heat production with AICAR treatment. All

data were tested for homogeneity of variances using Levene's test. Data were ln transformed when Levene's test was significant. In cases where transformed data also failed Levene's test, we used Kruskal–Wallis one-way ANOVA on ranks. The significance was considered as  $P < 0.05$ .

## RESULTS

### AMPK and ACC concentration during development

In liver, the mRNA concentrations of the AMPK $\alpha$ 1 and  $\beta$ 2 subunits were significantly elevated before hatching (-3) compared with at later developmental stages ( $\alpha$ 1,  $F_{3,20}=3.911$ ,  $P < 0.03$ ; Fig. 1A;  $\beta$ 2,  $F_{3,20}=7.138$ ,  $P < 0.003$ ; Fig. 1B). By contrast, AMPK  $\gamma$ 1 mRNA levels increased significantly after hatching (+1) in liver ( $F_{3,20}=8.649$ ,  $P < 0.001$ ; Fig. 1C). Phosphorylation of AMPK was elevated after hatching (+8) compared with at earlier developmental stages ( $H_{3,28}=8.703$ ,  $P < 0.05$ ; Fig. 1D), paralleling an increase in total AMPK protein content across this developmental period ( $F_{3,28}=3.068$ ,  $P < 0.05$ ; Fig. 1E). Phosphorylated and total ACC protein content was also elevated after hatching (+8) compared with at earlier developmental stages (pACC,  $H_{3,28}=25.61$ ,  $P < 0.0001$ ; Fig. 1F; total ACC,  $H_{3,28}=20.91$ ,  $P < 0.0002$ ; Fig. 1G).

In skeletal muscle, the mRNA concentration of the AMPK  $\alpha$ 2 subunit remained constant ( $F_{3,20}=0.28$ ,  $P > 0.8$ ; Fig. 2A). However,

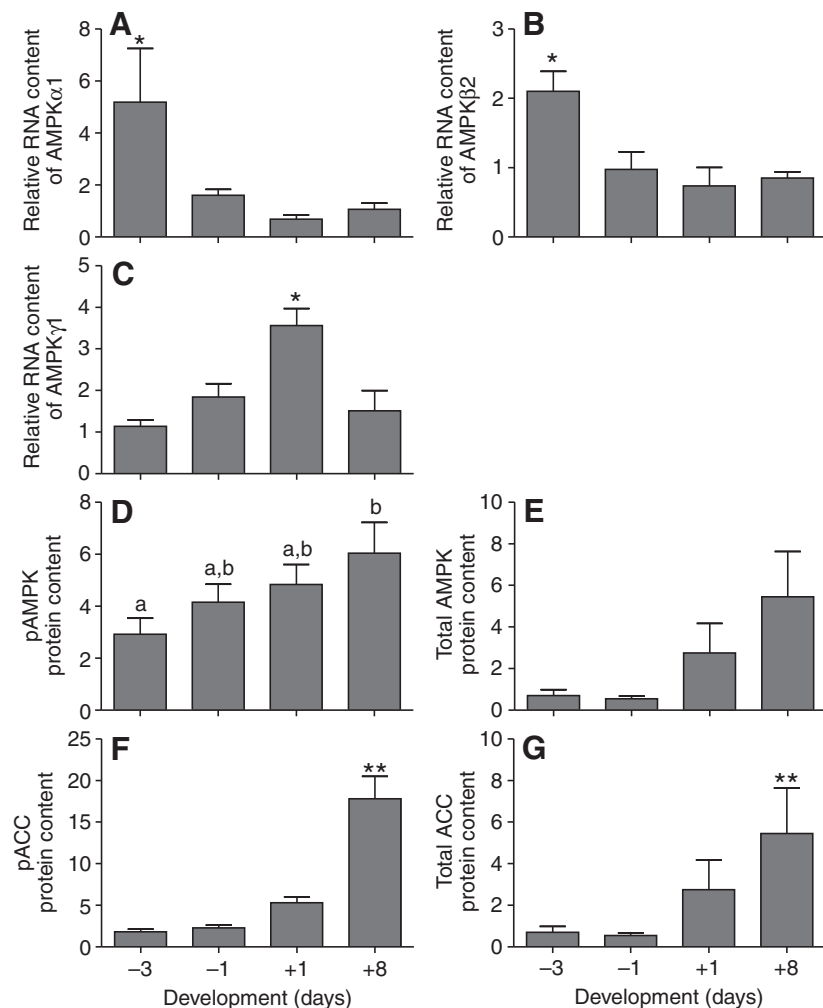


Fig. 1. AMP-activated protein kinase (AMPK) and acetyl CoA carboxylase (ACC) concentration during development in liver (means ± s.e.m.). Before hatching (-3 days), the relative mRNA concentration of AMPK $\alpha$ 1 (A) and  $\beta$ 2 (B) subunits was significantly increased, and the mRNA concentration of AMPK  $\gamma$ 1 (C) increased significantly after hatching (+1 day). These animals are endothermic by day 8 after hatching. RNA data (A-C) are expressed as relative to adult mRNA levels. AMPK and ACC activity (D,F), measured as phosphorylated protein content, as well as the total protein content of AMPK and ACC (E,G), were significantly elevated after hatching. Protein data (D-G) were normalized against 14-3-3 within each experiment. \*,  $P < 0.05$ ,  $> 0.001$ ; \*\*,  $P < 0.001$ ; same letters samples are not significantly different from each other ( $P > 0.05$ ); different letters samples are significantly different from one another ( $P < 0.05$ ).

AMPK  $\beta 2$  and  $\gamma 3$  mRNA levels increased significantly after hatching ( $\beta 2$ ,  $F_{3,20}=9.43$ ,  $P<0.001$ ; Fig. 2B;  $\gamma 3$ ,  $F_{3,20}=41.66$ ,  $P<0.0001$ ; Fig. 2C). There was no significant change in pAMPK or total AMPK concentration during development (pAMPK,  $F_{3,28}=2.446$ ,  $P>0.08$ ; Fig. 2D; total AMPK,  $F_{3,28}=0.849$ ,  $P>0.4$ ; Fig. 2E).

#### Acute AMPK activation

In liver, a single dose of  $1\text{ mg g}^{-1}$  AICAR significantly increased AMPK phosphorylation compared with control and  $0.5\text{ mg g}^{-1}$  AICAR groups ( $F_{2,23}=18.575$ ,  $P<0.001$ ; Fig. 3A). PGC-1 $\alpha$  and NRF-1 mRNA levels remained unchanged after AICAR treatment ( $1\text{ mg g}^{-1}$ ) compared with the control group (PGC-1 $\alpha$ ,  $t_{10}=-1.152$ ,  $P>0.1$ ; NRF-1,  $t_{5,882}=0.831$ ,  $P>0.2$ ; data not shown).

In skeletal muscle, neither concentration of AICAR changed AMPK phosphorylation. Also, total AMPK concentration remained constant (pAMPK,  $F_{2,23}=0.816$ ,  $P>0.4$ ; Fig. 3B; total AMPK,  $F_{2,23}=2.352$ ,  $P>0.1$ ; Fig. 3C). As in liver, the mRNA concentration of PGC-1 $\alpha$  and NRF-1 remained unchanged after AICAR treatment ( $1\text{ mg g}^{-1}$ ) compared with the control group (PGC-1 $\alpha$ ,  $t_{10}=-0.869$ ,  $P>0.2$ ; NRF-1,  $t_{10}=0.131$ ,  $P>0.4$ ; data not shown).

#### Chronic AMPK activation

The body mass of embryos one day before hatching (day -1; AICAR,  $48.53\pm 1.05\text{ g}$ ; control,  $51.42\pm 2.52\text{ g}$ ) and one day after hatching (day +1; AICAR,  $49.16\pm 1.33\text{ g}$ ; control,  $47.36\pm 0.77\text{ g}$ ) was not significantly different between AICAR and control groups (embryos,  $t_{9,410}=1.057$ ,  $P>0.1$ ; hatchlings,  $t_{12,817}=-1.179$ ,  $P>0.1$ ). AICAR treatment caused a significant decrease in plasma glucose in embryos ( $t_{15}=2.633$ ,  $P<0.02$ ; Fig. 4) and in hatchlings ( $t_{16}=3.333$ ,  $P<0.005$ ; Fig. 4).

In liver, chronic AICAR treatment increased pAMPK compared with the control, to a level that only reached statistical significance in hatchlings (-1,  $t_{14}=1.6$ ,  $P>0.1$ ; Fig. 5A; +1,  $t_{14}=3.42$ ,  $P<0.005$ ; Fig. 5C). Total AMPK concentration did not change with treatment either before ( $t_{14}=1.32$ ,  $P>0.1$ ; Fig. 5B) or after ( $t_{14}=0.49$ ,  $P>0.1$ ; Fig. 5D) hatching. In skeletal muscle, chronic AICAR treatment significantly increased AMPK phosphorylation before ( $t_{14}=2.66$ ,  $P<0.03$ ; Fig. 5E) and after ( $t_{14}=2.78$ ,  $P<0.02$ ; Fig. 5G) hatching, with total AMPK concentration remaining constant (-1d,  $t_{14}=-0.91$ ,  $P>0.1$ ; Fig. 5F; +1d,  $t_{14}=-0.72$ ,  $P>0.1$ ; Fig. 5H).

Chronic AMPK activation significantly increased heat production before ( $t_{15}=-3.888$ ,  $P<0.002$ ; Fig. 6A) and after ( $t_{10}=-2.266$ ,  $P<0.05$ ; Fig. 6B) hatching compared with the control groups. In liver, chronic AICAR treatment had no effect on citrate synthase (CS) activity before hatching ( $t_{14}=-0.582$ ,  $P>0.1$ ; Fig. 6C), but significantly increased CS activity after hatching compared with the control group ( $t_{14}=2.772$ ,  $P<0.02$ ; Fig. 6C). In skeletal muscle, chronic AMPK activation decreased CS activity before hatching ( $t_{14}=-2.176$ ,  $P<0.05$ ; Fig. 6D), but CS activity increased after hatching in the AICAR treatment group compared with the control group ( $t_{9,675}=5.304$ ,  $P<0.001$ ; Fig. 6D). Cytochrome-c oxidase (COX) activity remained unchanged after AICAR treatment compared with the control group before and after hatching in liver (before,  $t_{14}=-1.698$ ,  $P>0.1$ ; after,  $t_{14}=0.736$ ,  $P>0.1$ ; data not shown) and in muscle (before,  $t_{8,216}=1.436$ ,  $P>0.1$ ; after,  $t_{14}=0.012$ ,  $P>0.1$ ; data not shown).

Chronic AMPK activation had no effect on PGC-1 $\alpha$  mRNA concentrations before hatching in liver ( $t_{14}=0.777$ ,  $P>0.1$ ; Fig. 7A) or in muscle ( $t_{14}=-0.976$ ,  $P>0.1$ ; Fig. 7B). By contrast, after hatching PGC-1 $\alpha$  mRNA concentration was significantly elevated in the AICAR group compared with the control group in muscle ( $t_{14}=2.536$ ,

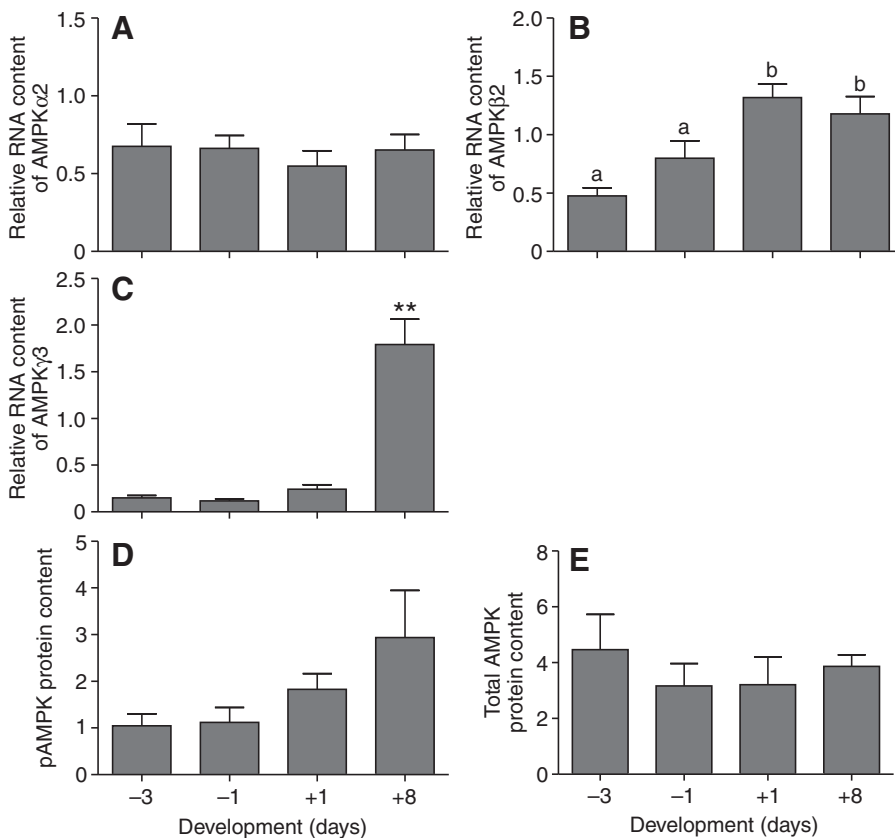


Fig. 2. AMPK concentration during development in skeletal muscle (means  $\pm$  s.e.m.). The relative mRNA concentration of AMPK $\alpha 2$  (A) remained stable during development, but the gene concentration of AMPK $\beta 2$  (B) and  $\gamma 3$  (C) increased significantly after hatching. These animals are endothermic by day 8 after hatching. All data are expressed as relative to adult mRNA levels. There was no significant change in AMPK phosphorylation (D) or total AMPK concentration (E) during development; protein data were normalized against 14-3-3 protein. \*,  $P<0.05$ ,  $>0.001$ ; \*\*,  $P<0.001$ ; same letters samples are not significantly different from each other ( $P>0.05$ ); different letters samples are significantly different from one another ( $P<0.05$ ).

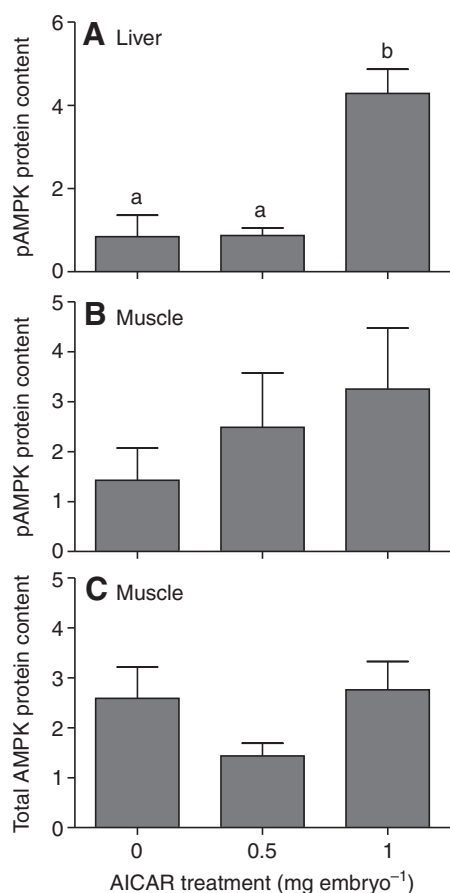


Fig. 3. AMPK phosphorylation in liver and skeletal muscle after acute AICAR treatment (means  $\pm$  s.e.m.). Samples were collected one hour after AICAR (5-aminoimidazole-4-carboxamide-1- $\beta$ -D-ribofuranoside) or control injection. A single dose of 1 mg g<sup>-1</sup> body mass AICAR increased AMPK phosphorylation in the liver (A) but not in skeletal muscle (B). Total AMPK concentration (C) remained unchanged after treatment in muscle. All protein data were normalized against 14-3-3 protein within each experiment. Same letters samples are not significantly different from each other ( $P>0.05$ ); different letters samples are significantly different from one another ( $P<0.05$ ).

$P<0.01$ ; Fig. 7B) and in liver ( $t_{14}=1.78$ ,  $P<0.05$ ; Fig. 7A). NRF-1 mRNA levels did not change with AICAR treatment in liver or muscle before (liver,  $t_{14}=-0.797$ ,  $P>0.1$ ; Fig. 7C; muscle,  $t_{14}=0.148$ ,  $P>0.1$ ; Fig. 7D) or after (liver,  $t_{9,69}=1.19$ ,  $P>0.1$ ; Fig. 7C; muscle,  $t_{14}=-0.88$ ,  $P>0.1$ ; Fig. 7D) hatching.

#### Induced hypothyroidism

In liver, hypothyroidism significantly reduced AMPK phosphorylation ( $t_{14}=3.090$ ,  $P<0.009$ ; Fig. 8A), despite an increase in total AMPK concentration in the methimazole treatment group compared with the control group ( $t_{14}=-2.990$ ,  $P<0.02$ ; Fig. 8B). In skeletal muscle, there was no significant difference between treatment groups in AMPK phosphorylation and total AMPK protein content (pAMPK,  $t_{14}=-0.816$ ,  $P>0.4$ ; Fig. 8C; total AMPK,  $t_{14}=-0.0138$ ,  $P>0.9$ ; Fig. 8D).

#### DISCUSSION

The development of endothermy during ontogenesis is accompanied by increasing ATP demands but reduced ATP synthesis efficiency (Walter and Seebacher, 2009). We show that AMPK plays a role

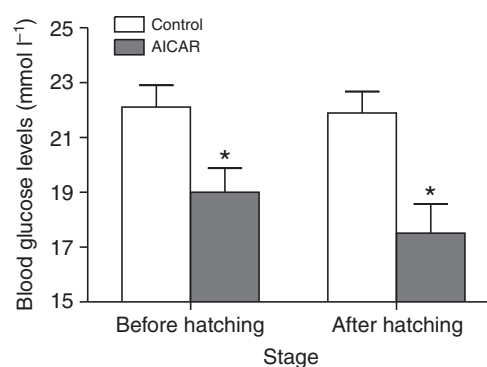


Fig. 4. Blood glucose levels (mmol l<sup>-1</sup>) after AICAR treatment. Chronic AICAR treatment (AICAR treatment, grey bars; control, white bars) significantly reduced blood glucose levels before and after hatching. \*,  $P<0.05$ ,  $>0.001$ .

in this process, and that increased phosphorylation of AMPK is associated with increased PGC-1 $\alpha$  concentrations and increased mitochondrial metabolic capacities. The increased mitochondrial abundance that is known to accompany the ontogenetic transition from ectothermy to endothermy can therefore be at least partly explained by the increase in AMPK phosphorylation and subsequent increase in PGC-1 $\alpha$  gene expression, a known inducer of mitochondrial biogenesis. These AMPK-mediated changes can contribute to the increased blood glucose utilization and heat production shown here. In addition, AMPK activity in liver is induced by thyroid hormone.

Both liver and muscle are important sites for metabolic heat production in endotherms (Rolfe and Brand, 1996; Rolfe et al., 1999; Ueda et al., 2005). Additionally, both have a high demand for ATP to sustain numerous housekeeping functions, such as gluconeogenesis in liver and contractile function in muscle. The increase in AMPK phosphorylation with development reflects the increasing demand for greater metabolic capacity to sustain both ATP-consuming functions and growth on the one hand, and heat production on the other. In skeletal muscle, the increase in AMPK phosphorylation after hatching paralleled that of liver, but the increase was not significant ( $P=0.08$ ). This non-significant result is due to the high variability among samples, which might reflect differences in the timing of the increase in muscle metabolic capacities between hatchlings. As a result of this variability, our sample size was too small to detect a statistical difference at  $P<0.05$ . The mRNA concentrations of all subunits changed during development, except for AMPK $\alpha$ 2 in muscle. However, there is no direct correspondence between mRNA and protein concentrations, which indicates that the assembly of the quaternary structure is not regulated by the mRNA concentration of any one subunit.

Mitochondrial proliferation is one of the key elements in the transition from ectothermy to endothermy, which is tightly linked to metabolic capacity (Seebacher et al., 2006). We show that, during the ontogenetic transition from ectothermy to endothermy in birds, activation of AMPK induces an increase in PGC-1 $\alpha$  mRNA concentration that is paralleled by an increase in mitochondrial content (CS activity) and heat production. These findings suggest that the previously observed increase in PGC-1 $\alpha$  and its target PPAR $\gamma$  in liver and skeletal muscle during the embryonic development of birds (Walter and Seebacher, 2007) is mediated by AMPK, and that AMPK plays a leading role in mitochondrial biogenesis by regulating PGC-1 $\alpha$  expression. AMPK regulates

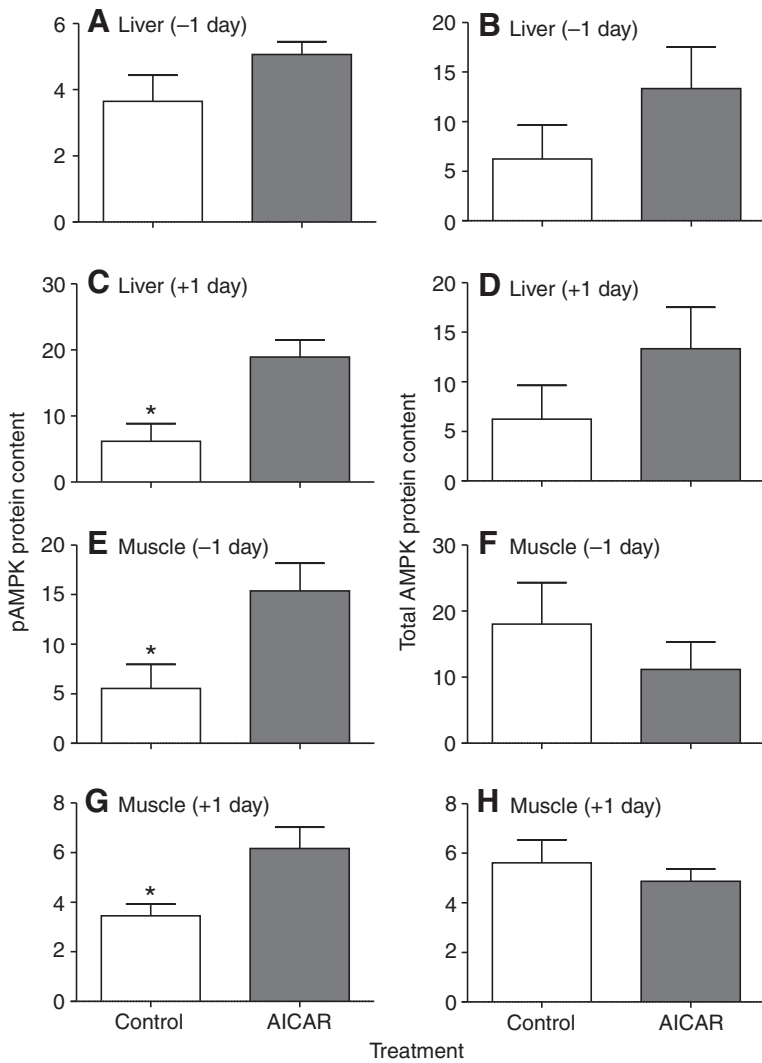


Fig. 5. AMPK phosphorylation in liver and skeletal muscle after chronic AICAR treatment (means  $\pm$  s.e.m.; AICAR treatment, grey bars; control, white bars). Samples were collected one day before and one day after hatching. In liver, following AICAR treatment, AMPK phosphorylation remained constant one day before hatching (A) but increased significantly after hatching (C). In skeletal muscle, chronic AICAR treatment significantly increased AMPK phosphorylation before (E) and after (G) hatching. Total AMPK concentration in liver (B,D) and muscle (F,H) did not change with treatment either before (B,F) or after (D,H) hatching. All protein data were normalized against 14-3-3 protein within each experiment. \*,  $P < 0.05$ ,  $> 0.001$ .

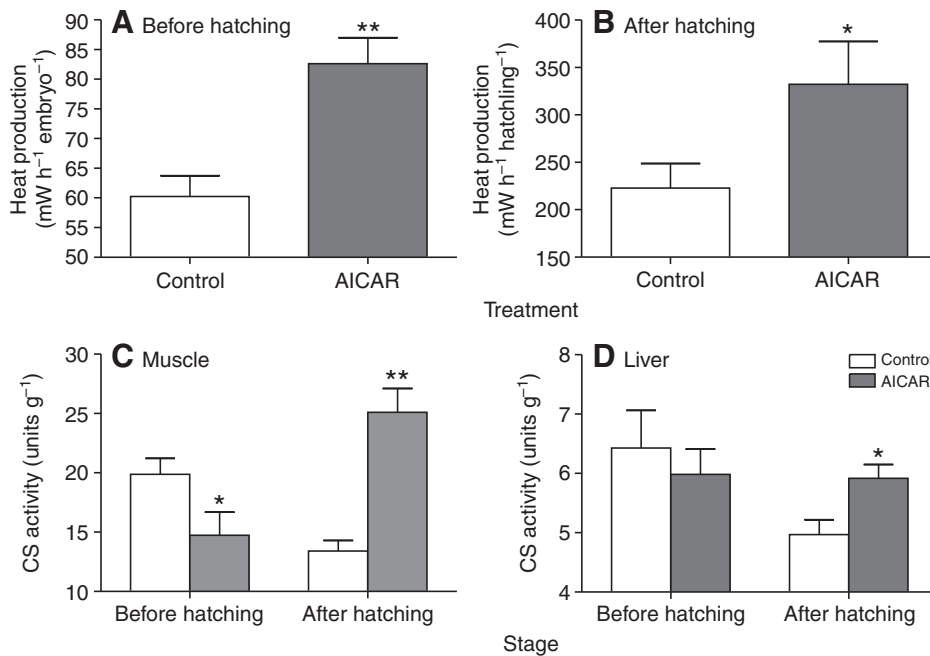


Fig. 6. Metabolic responses of liver and skeletal muscle to chronic AICAR treatment (means  $\pm$  s.e.m.; treatment, grey bars; control, white bars). AICAR treatment significantly increased heat production, measured as resting oxygen consumption, one day before (A) and one day after (+1; B) hatching. In liver (C), citrate synthase (CS) activity remained constant before hatching but significant increased after hatching. In skeletal muscle (D), chronic AICAR treatment decreased CS activity before hatching, but CS activity increased significantly after hatching. \*,  $P < 0.05$ ,  $> 0.001$ ; \*\*,  $P < 0.001$ .

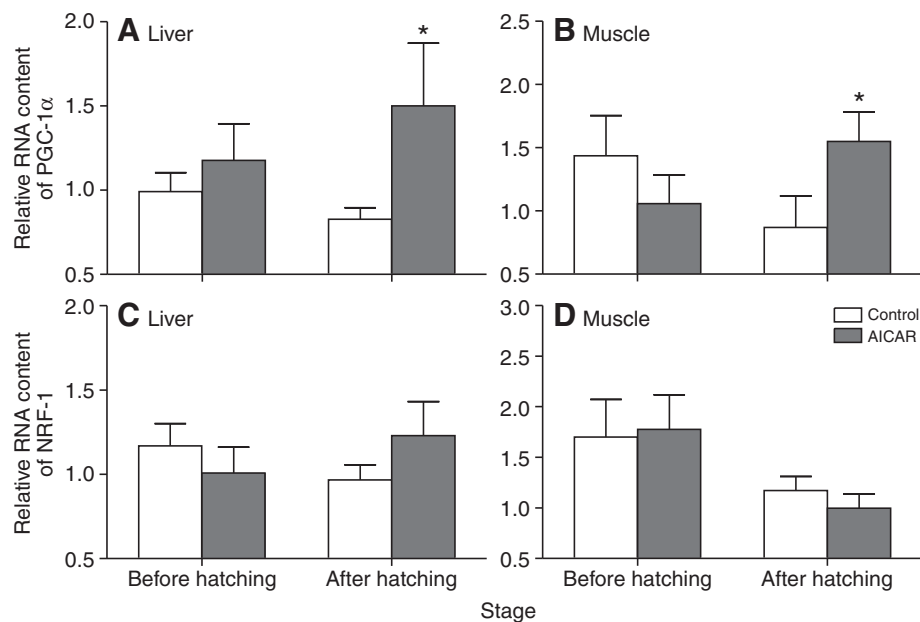


Fig. 7. Transcriptional regulators in liver and skeletal muscle after chronic AICAR treatment (means  $\pm$  s.e.m.; treatment, grey bars; control, white bars). Relative mRNA concentration of the PGC-1 $\alpha$  gene remained constant with treatment before hatching but was significantly increased in the treatment group after hatching in liver (A) and skeletal muscle (B). NRF-1 gene concentration remained constant with treatment in liver (C) and skeletal muscle (D). \*,  $P < 0.05$ ,  $> 0.001$ ; \*\*,  $P < 0.001$ .

PGC-1 $\alpha$  expression either directly by phosphorylating PGC-1 $\alpha$  (Jager et al., 2007), or indirectly by activating SIRT1. SIRT1 is a NAD1-dependent type III deacetylase (Canto et al., 2009; Nemoto et al., 2005), which stimulates the PGC-1 $\alpha$ -dependent induction of the PGC-1 $\alpha$  promoter (note that PGC-1 $\alpha$  can regulate its own promoter). PGC-1 $\alpha$  interacts with a suite of transcription factors, such as NRF-1 and NRF-2, to control mitochondrial biogenesis (Finck and Kelly, 2006; Scarpulla, 2008). NRF-1 mRNA was not affected by AICAR treatment, which indicates that AMPK does not influence NRF-1 gene expression. The significant decrease in muscle CS activity of control animals after hatching is likely to reflect hypertrophy and the consequent decrease in mitochondrial density per unit tissue of muscle cells that is associated with the onset of locomotion. The decrease in CS activity disappears four

days after hatching (Walter and Seebacher, 2007), indicating that mitochondrial proliferation follows hypertrophy.

There are strong similarities between the action of AMPK during bird development and its role in metabolic regulation in response to exercise and diet in mammals (Park et al., 2002; Viollet et al., 2009b). Hence, in mammals AMPK is known to promote mitochondrial biogenesis by interacting with PGC-1 $\alpha$ , NRF-1, NRF-2 and mitochondrial transcription factor A in response to exercise or metabolic stress (Viollet et al., 2009a). In the liver of mammals, AMPK regulates cellular energy homeostasis by controlling mitochondrial biogenesis (Guigas et al., 2007). Hepatocytes from AMPK $\alpha 1\alpha 2_{LS}^{-/-}$  mice, which lack both  $\alpha 1$  and  $\alpha 2$  AMPK catalytic subunits, show a decreased oxidative capacity that is linked to a decreased cellular density of mitochondria as a result of decreased

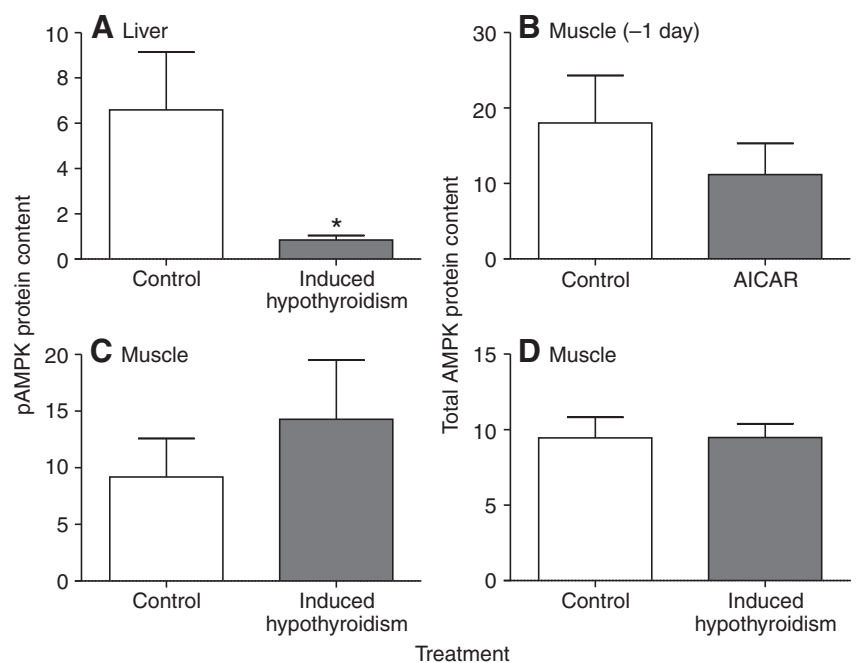


Fig. 8. Effect of induced hypothyroidism on AMPK phosphorylation in liver and skeletal muscle (means  $\pm$  s.e.m.; methimazole treatment, grey bars; control, white bars). Hypothyroidism significantly reduced AMPK phosphorylation in liver (A) but not in skeletal muscle (C). Total AMPK protein content of the hypothyroid group was significantly increased in liver (B), but did not change with treatment in skeletal muscle (D). Protein data were normalized against 14-3-3 protein within each experiment. \*,  $P < 0.05$ ,  $> 0.001$ ; \*\*,  $P < 0.001$ .

expression of PGC-1 $\alpha$ , COX subunit I (COXI) and Fo/F1 ATPase (Guigas et al., 2007). Similarly, non-exercised red and white gastrocnemius muscles of AMPK $\alpha$ 2<sup>-/-</sup> mice show a 20% reduction in mitochondrial markers such as COXI protein content and CS activity (Jorgensen et al., 2007). Interestingly, a double knockout of catalytic AMPK subunits (AMPK $\alpha$ 1 and AMPK $\alpha$ 2) in embryonic mice is lethal at ~10.5 days post-conception (Viollet et al., 2009a), which demonstrates the importance of AMPK in controlling energy metabolism during development. Additionally, AMPK has been suggested to mediate normal metabolic development of human neonates, and in particular the switch from glycolytic to oxidative metabolism, by regulating glucose and fatty acid metabolism (Brauner et al., 2006). These data together with our findings show that there are similarities in the pathways that regulate the ontogenetic transition from ectothermy to endothermy in birds and mammals. However, unlike in mammals, NRF-1 in birds does not respond to AICAR treatment and it is therefore unlikely to be involved in the AMPK-mediated metabolic responses.

In addition to its function in modulating mitochondrial biogenesis, AMPK controls the coordination of lipid metabolism by balancing fatty acid oxidation with long-chain fatty acid synthesis (Viollet et al., 2009b). In chicken, lipogenesis occurs only after hatching, because the embryo directly derives fatty acids from yolk lipids (Ryder, 1970). The increase in ACC indicates increased lipogenesis in the liver (Carling et al., 1987) of hatchlings that is inhibited by increasing AMPK phosphorylation, which thereby balances fat storage with ATP and heat production in mitochondria.

The decrease in blood glucose levels after AICAR treatment shows, firstly, an involvement of AMPK on whole-body glucose homeostasis during development and, secondly, the increasing energy demands caused among others by elevated mitochondrial biogenesis. Also, AICAR might possibly affect other AMP-sensitive enzymes, such as fructose-1, 6-bisphosphatase, that influence blood glucose levels independently of AMPK (Vincent et al., 1991). However, in mammals AMPK regulates glucose uptake. For example, in the liver of AMPK $\alpha$ 1 $\alpha$ 2<sub>LS</sub><sup>-/-</sup> mice, up to 40% of AICAR-induced hypoglycemia is due to the activation of AMPK (Viollet et al., 2009b). Hepatic glucose production is the primary mechanism for regulating glucose flux at rest and, in mammals, liver AMPK is important in maintaining whole-body glucose homeostasis by inhibiting hepatic glucose production if energy demands increase (Foretz et al., 2005; Viollet et al., 2009a). If circulating glucose levels do not meet metabolic energy demand, the liver releases glucose by glycogenolysis, and in the longer term by gluconeogenesis (Hegarty et al., 2009). Furthermore, because the growing embryo has only a limited energy supply (the yolk), decreasing blood glucose levels cannot be replenished. AMPK plays a role in gluconeogenesis because of its capacity to control the expression of some key gluconeogenic genes (e.g. PEPCK and G6Pase) by phosphorylating the CREB co-activator TORC2 (Koo et al., 2005; Viollet et al., 2009b). Similarly, in muscle AMPK stimulates beta oxidation and glucose utilization, which leads to an increase in metabolic capacity. Furthermore, AMPK regulates skeletal muscle capillarization and VEGF expression (Zwetsloot et al., 2008), which assures sufficient vascularization to provide substrates to sustain increased metabolic activity (Adair, 2005).

Thyroid hormones are known to play an important role in regulating the mitochondrial metabolism and internal heat production of endotherms (Lowell and Spiegelman, 2000; Silva, 1995). This effect is at least partly due to increased fatty acid oxidation *via* the AMPK-mediated inhibition of ACC (de Lange et al., 2008; Lombardi et al., 2009). Here we show that, in addition to blocking ACC, thyroid

hormone also alters the phosphorylation state of AMPK and thereby causes an increase in PGC-1 $\alpha$  gene expression during development. We have previously shown that T3 regulates mitochondrial function and capacity *via* PGC-1 $\alpha$  during the development of endothermy (Walter and Seebacher, 2009). Those results can now be explained by a direct genomic effect of thyroid hormone on PGC-1 $\alpha$  gene expression and by its effect *via* AMPK phosphorylation.

In conclusion, even though modern endotherms, mammals and birds, are phylogenetically distinct, AMPK signalling appears to be a common and conserved molecular mechanism that controls metabolic heat production. Our data suggest that, as in mammals, the ontogenetic transition from ectothermy to endothermy in birds is controlled by thyroid hormones that stimulate AMPK to induce PGC-1 $\alpha$  expression. Consequently, as in mammals, this kinase plays a role in regulating mitochondrial biogenesis. Thus, increases in mitochondrial content lead towards an enhanced ATP production to support the growing organism, as well as to increased internal heat production. It will be interesting for future research to investigate the importance of AMPK in controlling energy demands, particularly in regulating Na<sup>+</sup>/K<sup>+</sup>-ATPase activity, that might drive increased metabolic flux through mitochondria (Walter and Seebacher, 2009). In mammalian lung epithelial cells, AMPK affects Na<sup>+</sup>/K<sup>+</sup>-ATPase activity if pharmacologically activated with metformin or AICAR under hypoxic conditions (Gusarova et al., 2009; Woollhead et al., 2007). If this interaction were generally true, AMPK would affect and control the main components of endothermy.

#### LIST OF ABBREVIATIONS

ACC	acetyl CoA carboxylase
AICAR	5-aminoimidazole-4-carboxamide-1- $\beta$ -D-ribofuranoside
AMPK	AMP-activated protein kinase
COX	cytochrome <i>c</i> oxidase
CS	citrate synthase

#### ACKNOWLEDGEMENTS

This work was supported by an Australian Research Council Discovery Grant to F.S.

#### REFERENCES

- Adair, T. H. (2005). Growth regulation of the vascular system: an emerging role for adenosine. *Am. J. Physiol. Regul. Integr. Comp. Physiol.* **289**, R283-R296.
- Bech, C., Martini, S., Brent, R. and Rasmussen, J. (1984). Thermoregulation in newly hatched black-legged kittiwakes. *Condor* **86**, 339-341.
- Bergeron, R., Ren, J. M., Cadman, K. S., Moore, I. K., Perret, P., Pypaert, M., Young, L. H., Semenkovich, C. F. and Shulman, G. I. (2001). Chronic activation of AMP kinase results in NRF-1 activation and mitochondrial biogenesis. *Am. J. Physiol. Endocrinol. Metab.* **281**, E1340-E1346.
- Brand, M. D., Couture, P., Else, P. L., Withers, K. W. and Hulbert, A. J. (1991). Evolution of energy-metabolism-proton permeability of the inner Membrane of liver-mitochondria is greater in a mammal than in a reptile. *Biochem. J.* **275**, 81-86.
- Brauner, P., Kopecky, P., Flachs, P., Kuda, O., Vorlicek, J., Planickova, L., Vitkova, I., Andreelli, F., Foretz, M., Viollet, B. et al. (2006). Expression of uncoupling protein 3 and GLUT4 gene in skeletal muscle of preterm newborns: Possible control by AMP-activated protein kinase. *Pediatr. Res.* **60**, 569-575.
- Canto, C., Gerhart-Hines, Z., Feige, J. N., Lagouge, M., Noriega, L., Milne, J. C., Elliott, P. J., Puigserver, P. and Auwerx, J. (2009). AMPK regulates energy expenditure by modulating NAD<sup>+</sup> metabolism and SIRT1 activity. *Nature* **458**, 1056-1060.
- Carling, D., Zammit, V. A. and Hardie, D. G. (1987). A common bicyclic protein-kinase cascade inactivates the regulatory enzymes of fatty-acid and cholesterol-biosynthesis. *FEBS Lett.* **223**, 217-222.
- Carling, D., Sanders, M. J. and Woods, A. (2008). The regulation of AMP-activated protein kinase by upstream kinases. *Int. J. Obes.* **32**, S55-S59.
- de Lange, P., Senese, R., Cioffi, F., Moreno, M., Lombardi, A., Silvestri, E., Gaglia, F. and Lanni, A. (2008). Rapid activation by 3,5,3'-L-triiodothyronine of adenosine 5'-monophosphate-activated protein kinase/acetyl-coenzyme A carboxylase and Akt/protein kinase B signaling pathways: relation to changes in fuel metabolism and myosin heavy-chain protein content in rat gastrocnemius muscle *in vivo*. *Endocrinology* **149**, 6462-6470.
- Decuyper, E. (1984). Incubation-temperature in relation to postnatal performance in chickens. *Arch. Exp. Veterinarmed.* **38**, 439-449.
- Decuyper, E., Nouwen, E. J., Kühn, E. R., Geers, R. and Michels, H. (1979). Iodohormones in the serum of chick embryos and post-hatching chickens as

- influenced by incubation temperature. Relationship with the hatching process and thermogenesis. *Ann. Biol. Anim. Biochim. Biophys.* **19**, 1713-1723.
- Else, P. L. and Hulbert, A. J.** (1987). Evolution of mammalian endothermic metabolism-leaky membranes as a source of heat. *Am. J. Physiol.* **253**, R1-R7.
- Finck, B. N. and Kelly, D. P.** (2006). PGC-1 coactivators: inducible regulators of energy metabolism in health and disease. *J. Clin. Invest.* **116**, 615-622.
- Foretz, M., Ancellin, N., Amdreilli, F., Saintillan, Y., Grondin, P., Kahn, A., Thorens, B., Vaulont, S. and Viollet, B.** (2005). Short-term overexpression of a constitutively active form of AMP-activated protein kinase in the liver leads to mild hypoglycemia and fatty liver. *Diabetes* **54**, 1331-1339.
- Guigas, B., Taleux, N., Foretz, M., Detaille, D., Amdreilli, F., Viollet, B. and Hue, L.** (2007). AMP-activated protein kinase-independent inhibition of hepatic mitochondrial oxidative phosphorylation by AICA riboside. *Biochem. J.* **404**, 499-507.
- Gusarova, G. A., Dada, L. A., Kelly, A. M., Brodie, C., Witters, L. A., Chandel, N. S. and Sznajder, J. I.** (2009).  $\alpha$ 1-AMP-Activated protein kinase regulates hypoxia-induced Na,K-ATPase endocytosis via direct phosphorylation of protein kinase C $\zeta$ . *Mol. Cell. Biol.* **29**, 3455-3464.
- Halseth, A. E., Ensor, N. J., White, T. A., Ross, S. A. and Gulve, E. A.** (2002). Acute and chronic treatment of ob/ob and db/db mice with AICAR decreases blood glucose concentrations. *Biochem. Biophys. Res. Commun.* **294**, 798-805.
- Hamburger, V. and Hamilton, H. L.** (1951). A series of normal stages in the development of the chick embryo. *J. Morphol.* **88**, 49-92.
- Hardie, D. G. and Carling, D.** (1997). The AMP-activated protein kinase-fuel gauge of the mammalian cell? *Eur. J. Biochem.* **246**, 259-273.
- Hegarty, B. D., Turner, N., Cooney, G. J. and Kraegen, E. W.** (2009). Insulin resistance and fuel homeostasis: the role of AMP-activated protein kinase. *Acta Physiol.* **196**, 129-145.
- Heldmaier, G.** (1975). Metabolic and thermoregulatory responses to heat and cold in djungarian hamster, *Phodopus sungorus*. *J. Comp. Physiol.* **102**, 115-122.
- Hoppeler, H.** (1986). Exercise-induced ultrastructural-changes in skeletal-muscle. *Int. J. Sports Med.* **7**, 187-204.
- Hou, C., Zuo, W. Y., Moses, M. E., Woodruff, W. H., Brown, J. H. and West, G. B.** (2008). Energy uptake and allocation during ontogeny. *Science* **322**, 736-739.
- Hoyt, D. F., Vleck, C. M. and Vleck, D.** (1978). Metabolism of avian embryos-ontogeny and temperature effects in ostrich. *Condor* **80**, 265-271.
- Hulbert, A. J. and Else, P. L.** (1990). The cellular basis of endothermic metabolism-a role for leaky membranes. *News Physiol. Sci.* **5**, 25-28.
- Irrcher, I., Adihetty, P. J., Sheehan, T., Joseph, A. M. and Hood, D. A.** (2003). PPAR gamma coactivator-1 alpha expression during thyroid hormone- and contractile activity-induced mitochondrial adaptations. *Am. J. Physiol. Cell Physiol.* **284**, C1669-C1677.
- Jager, S., Handschin, C., Pierre, J. and Spiegelman, B. M.** (2007). AMP-activated protein kinase (AMPK) action in skeletal muscle via direct phosphorylation of PGC-1 alpha. *Proc. Natl. Acad. Sci. USA* **104**, 12017-12022.
- Jorgensen, S. B., Trebak, J. T., Viollet, B., Schjerling, P., Vaulont, S., Wojtaszewski, J. F. P. and Richter, E. A.** (2007). Role of AMPK $\alpha$ 2 in basal, training-, and AICAR-induced GLUT4, hexokinase II, and mitochondrial protein expression in mouse muscle. *Am. J. Physiol. Endocrinol. Metab.* **292**, E331-E339.
- Kahn, B. B., Alquier, T., Carling, D. and Hardie, D. G.** (2005). AMP-activated protein kinase: Ancient energy gauge provides clues to modern understanding of metabolism. *Cell Metab.* **1**, 15-25.
- Klaassen, M., Slagsvold, G. and Bech, C.** (1987). Metabolic rate and thermostability in relation to availability of yolk in hatchlings of black-legged kittiwake and domestic chicken. *Auk* **104**, 787-789.
- Koo, S. H., Flechner, L., Qi, L., Zhang, X. M., Sreaton, R. A., Jeffries, S., Hedrick, S., Xu, W., Boussouar, F., Brindle, P. et al.** (2005). The CREB coactivator TORC2 is a key regulator of fasting glucose metabolism. *Nature* **437**, 1109-1114.
- Kooijman, S., Sousa, T., Pecquerie, L., van der Meer, J. and Jager, T.** (2008). From food-dependent statistics to metabolic parameters, a practical guide to the use of dynamic energy budget theory. *Biol. Rev.* **83**, 533-552.
- Lombardi, A., de Lange, P., Silvestri, E., Busiello, R. A., Lanni, A., Goglia, F. and Moreno, M.** (2009). 3,5-Diiodo-L-thyronine rapidly enhances mitochondrial fatty acid oxidation rate and thermogenesis in rat skeletal muscle: AMP-activated protein kinase involvement. *Am. J. Physiol. Endocrinol. Metab.* **296**, E497-E502.
- Lowell, B. B. and Spiegelman, B. M.** (2000). Towards a molecular understanding of adaptive thermogenesis. *Nature* **404**, 652-660.
- Nemoto, S., Fergusson, M. M. and Finkel, T.** (2005). SIRT1 functionally interacts with the metabolic regulator and transcriptional coactivator PGC-1 alpha. *J. Biol. Chem.* **280**, 16456-16460.
- Park, H., Kaushik, V. K., Constant, S., Prentki, M., Przybytkowski, E., Ruderman, N. B. and Saha, A. K.** (2002). Coordinate regulation of malonyl-CoA decarboxylase, sn-glycerol-3-phosphate acyltransferase, and acetyl-CoA carboxylase by AMP-activated protein kinase in rat tissues in response to exercise. *J. Biol. Chem.* **277**, 32571-32577.
- Pfaffl, M. W.** (2001). A new mathematical model for relative quantification in real-time RT-PCR. *Nucleic Acids Res.* **29**, e45.
- Proszkowiec-Weglarz, M. and Richards, M. P.** (2007). 5'-AMP-activated protein kinase in avian biology. *Avian Poult. Biol. Rev.* **18**, 123-145.
- Proszkowiec-Weglarz, M. and Richards, M. P.** (2009). Expression and activity of the 5'-adenosine monophosphate-activated protein kinase pathway in selected tissues during chicken embryonic development. *Poult. Sci.* **88**, 159-178.
- Puigserver, P. and Spiegelman, B. M.** (2003). Peroxisome proliferator-activated receptor-gamma coactivator 1 alpha (PGC-1 alpha): Transcriptional coactivator and metabolic regulator. *Endocr. Rev.* **24**, 78-90.
- Reznick, R. M. and Shulman, G. I.** (2006). The role of AMP-activated protein kinase in mitochondrial biogenesis. *J. Physiol.* **574**, 33-39.
- Rolfe, D. F. and Brand, M. D.** (1996). Contribution of mitochondrial proton leak to skeletal muscle respiration and to standard metabolic rate. *Am. J. Physiol. Cell Physiol.* **271**, C1380-C1389.
- Rolfe, D. F. S., Newman, J. M. B., Buckingham, J. A., Clark, M. G. and Brand, M. D.** (1999). Contribution of mitochondrial proton leak to respiration rate in working skeletal muscle and liver and to SMR. *Am. J. Physiol. Cell Physiol.* **276**, C692-C699.
- Ryder, E.** (1970). Effect of development on chicken liver acetyl-coenzyme-a carboxylase. *Biochem. J.* **119**, 929-930.
- Sanders, M. J., Grondin, P. O., Hegarty, B. D., Snowden, M. A. and Carling, D.** (2007). Investigating the mechanism for AMP activation of the AMP-activated protein kinase cascade. *Biochem. J.* **403**, 139-148.
- Scarpulla, R. C.** (2008). Transcriptional paradigms in mammalian mitochondrial biogenesis and function. *Physiol. Rev.* **88**, 611-638.
- Seebacher, F., Guderley, H., Eisey, R. M. and Troscclair, P. L., III** (2003). Seasonal acclimatization of muscle metabolic enzymes in a reptile (*Alligator mississippiensis*). *J. Exp. Biol.* **206**, 1193-1200.
- Seebacher, F., Schwartz, T. S. and Thompson, M. B.** (2006). Transition from ectothermy to endothermy: the development of metabolic capacity in a bird (*Gallus gallus*). *Proc. R. Soc. Lond. B. Biol. Sci.* **273**, 565-570.
- Silva, J. E.** (1995). Thyroid hormone control of thermogenesis and energy balance. *Thyroid* **5**, 481-492.
- Tzschentke, B. and Nichelmann, M.** (1999). Development of avian thermoregulatory system during the early postnatal period: development of the thermoregulatory set-point. *Ornis Fennica* **76**, 189-198.
- Ueda, M., Watanabe, K., Sato, K., Akiba, Y. and Toyomizu, M.** (2005). Possible role for avPGC-1 $\alpha$  in the control of expression of fiber type, along with avUCP and avANT mRNAs in the skeletal muscles of cold-exposed chickens. *FEBS Lett.* **579**, 11-17.
- Vincent, M. F., Marangos, P. J., Gruber, H. E. and Van den Berghe, G.** (1991). Inhibition by AICA riboside of gluconeogenesis in isolated rat hepatocytes. *Diabetes* **40**, 1259-1266.
- Viollet, B., Athea, Y., Mounier, R., Guigas, B., Zarrinpashneh, E., Horman, S., Lantier, L., Hebrard, S., Devin-Leclerc, J., Beauloye, C. et al.** (2009a). AMPK: Lessons from transgenic and knockout animals. *Front. Biosci.* **14**, 19-44.
- Viollet, B., Guigas, B., Leclerc, J., Hébrard, S., Lantier, L., Mounier, R., Amdreilli, F. and Foretz, M.** (2009b). AMP-activated protein kinase in the regulation of hepatic energy metabolism: from physiology to therapeutic perspectives. *Acta Physiol.* **196**, 81-98.
- Walter, I. and Seebacher, F.** (2007). Molecular mechanisms underlying the development of endothermy in birds (*Gallus gallus*): a new role of PGC-1 $\alpha$ ? *Am. J. Physiol. Regul. Integr. Comp. Physiol.* **293**, R2315-R2322.
- Walter, I. and Seebacher, F.** (2009). Endothermy in birds: underlying molecular mechanisms. *J. Exp. Biol.* **212**, 2328-2336.
- Winder, W. and Thomson, D.** (2007). Cellular energy sensing and signaling by AMP-activated protein kinase. *Cell Biochem. Biophys.* **47**, 332-347.
- Winder, W. W., Holmes, B. F., Rubink, D. S., Jensen, E. B., Chen, M. and Holloszy, J. O.** (2000). Activation of AMP-activated protein kinase increases mitochondrial enzymes in skeletal muscle. *J. Appl. Physiol.* **88**, 2219-2226.
- Woolhead, A. M., Sivagnanasundaram, J., Kalsi, K. K., Pucovsky, V., Pellatt, L. J., Scott, J. W., Mustard, K. J., Hardie, D. G. and Baines, D. L.** (2007). Pharmacological activators of AMP-activated protein kinase have different effects on Na<sup>+</sup> transport processes across human lung epithelial cells. *Br. J. Pharmacol.* **151**, 1204-1215.
- Wu, B. J., Hulbert, A. J., Storlien, L. H. and Else, P. L.** (2004). Membrane lipids and sodium pumps of cattle and crocodiles: an experimental test of the membrane pacemaker theory of metabolism. *Am. J. Physiol. Regul. Integr. Comp. Physiol.* **287**, R633-R641.
- Zong, H., Ren, J. M., Young, L. H., Pypaert, M., Mu, J., Birnbaum, M. J. and Shulman, G. I.** (2002). AMP kinase is required for mitochondrial biogenesis in skeletal muscle in response to chronic energy deprivation. *Proc. Natl. Acad. Sci. USA* **99**, 15983-15987.
- Zwetsloot, K. A., Westerkamp, L. M., Holmes, B. F. and Gavin, T. P.** (2008). AMPK regulates basal skeletal muscle capillarization and VEGF expression, but is not necessary for the angiogenic response to exercise. *J. Physiol.* **586**, 6021-6035.